Journal of Physics and Chemistry of Solids 114 (2018) 88–93

Contents lists available at ScienceDirect

Journal of Physics and Chemistry of Solids

journal homepage: www.elsevier.com/locate/jpcs

Fluorescence and afterglow of $Ca_2Sn_2Al_2O_9$:Mn^{2+}

Minoru Takemoto *, Takahiro Iseki

Department of Applied Chemistry, Faculty of Engineering, Kanagawa Institute of Technology, 1030 Shimo-Ogino, Atsugi, Kanagawa 243-0292, Japan

ARTICLE INFO

Keywords:
A. oxides
C. X-ray diffraction
D. crystal structure
D. luminescence

ABSTRACT

By using a polymerized complex method, we synthesized manganese (Mn)-doped $Ca_2Sn_2Al_2O_9$, which exhibits yellow fluorescence and afterglow at room temperature when excited by UV radiation. The material emits a broad, featureless fluorescence band centered at 564 nm, which we attribute to the presence of Mn^{2+} ions. The afterglow decay is well fit by a power-law function, rather than an exponential function. In addition, thermoluminescence analyses demonstrate that two different types of electron traps form in this material. Based on experimental results, we conclude that the fluorescence and afterglow both result from thermally assisted tunneling, in which trapped electrons are thermally excited to higher-level traps and subsequently tunnel to recombination centers.

1. Introduction

Divalent manganese ions, Mn^{2+}, are known to emit light as a result of the electronic transition from the $^4T_1$ (^4G) electronic state to the $^6A_1$ (^6S) ground state. According to the Tanabe–Sugano diagram for this ion [1], the energy of the $^4T_1$ (^1G) state decreases as the Mn^{2+} crystal field increases, which means that the fluorescent color generated by Mn^{2+} ions depends on the host crystal. Various Mn^{2+}-activated fluorescent materials have been developed, exhibiting a variety of colors: Mg_2SnO_4:Mn^{2+} (with an emission wavelength of 499 nm) [2], $ZnGa_2O_4$:Mn^{2+} (506 nm) [3], $ZnAl_2O_4$:Mn^{2+} (513 nm) [4], Zn_2SiO_4:Mn^{2+} (523 nm) [5], CaZnOS:Mn^{2+} (614 nm) [6], BaZnOS:Mn^{2+} (634 nm) [6], $CaZnGe_2O_6$:Mn^{2+} (648 nm) [7], and $MgGeO_3$:Mn^{2+} (670 nm) [8]. Recently, many phosphors have been developed by co-doping with Mn^{2+} in combination with lanthanide ions, such as Ce^{3+}. Examples of phosphors include $Ca_5(PO_4)_3F$:Ce^{3+},Mn^{2+} [9], $Ca_9Y(PO_4)_7$:Ce^{3+},Mn^{2+} [10], $Ca_3Sc_2Si_3O_{12}$:Ce^{3+},Mn^{2+} [11], $M_5(PO_4)_3Cl$ (M = Ca, Sr):Eu^{2+},Mn^{2+} [12], $Sr_3La(PO_4)_3$:Eu^{2+},Mn^{2+} [13], $Ca_9MgK(PO_4)_7$:Eu^{2+},Mn^{2+} [14], $LaMgAl_{11}O_{19}$:Tb^{3+},Mn^{2+} [15], $ZnAl_2O_4$:Tb^{3+},Mn^{2+} [16], and $NaCaPO_4$:Tb^{3+},Mn^{2+} [17]. In these phosphors, the Mn^{2+} ions emit light following energy transfer from the lanthanide ions to the Mn^{2+} ions.

As described above, Mn^{2+} ions are very important as light emitters. Thus, in developing novel phosphors based on Mn^{2+} doping, it is important to select host crystals that have sites which Mn^{2+} can occupy. One such candidate is calcium tin aluminate with the composition $Ca_2Sn_2Al_2O_9$, which has been synthesized and its crystal structure refined [18]. This structure is presented in Fig. 1 and consists of edge-sharing $[CaO_7]^{12-}$ and $[SnO_6]^{8-}$ polyhedra that form a double layer, with interlayer $[AlO_4]^{5-}$ polyhedral layers connecting adjacent double layers. The ionic radii [19] of the constituent metals are Ca^{2+} = 0.106 nm (coordination number CN = VII), Sn^{4+} = 0.069 nm (VI), and Al^{3+} = 0.039 nm (IV). In the high-spin state, the ionic radii of Mn^{2+} are 0.09 nm (CN = VII), 0.083 nm (VI), and 0.066 nm (IV). Comparing the radius and valence state of the constituent metal ions with those of Mn^{2+} clearly indicates that Mn^{2+} ions doped into a $Ca_2Sn_2Al_2O_9$ host crystal will likely occupy Ca^{2+} sites. In this work, we find that doping $Ca_2Sn_2Al_2O_9$ samples solely with Mn^{2+} leads to yellow fluorescence and afterglow at room temperature during and after UV irradiation, respectively. Because afterglow in phosphor crystals typically originates from electron traps that in turn result from crystal defects, we anticipated that a detailed investigation of these samples would reveal not only the fluorescence characteristics of Mn^{2+} but also the nature of the electron traps in the $Ca_2Sn_2Al_2O_9$ host crystal. With this motivation, we assessed in detail the fluorescent properties of $Ca_2Sn_2Al_2O_9$ doped with Mn^{2+}.

2. Experiment

The samples with the chemical composition of $(Ca_{2-x}Mn_x)Sn_2Al_2O_9$ were synthesized by using a polymerized complex method utilized by Nakamura et al. [20]. $CaCO_3$ (99.99%), $SnCl_4{\cdot}5H_2O$ (98.0%), $Al(NO_3)_3{\cdot}9H_2O$ (99.9%), and $Mn(CH_3COO)_2{\cdot}4H_2O$ (99.9%) were used as starting materials and were dissolved in aqueous nitric acid in the appropriate quantities. Citric acid and propylene glycol were subsequently added to the solution and the mixture was heated to 363 K and

---

* Corresponding author.
E-mail address: takemoto@chem.kanagawa-it.ac.jp (M. Takemoto).

https://doi.org/10.1016/j.jpcs.2017.11.016
Received 28 August 2017; Received in revised form 11 November 2017; Accepted 18 November 2017

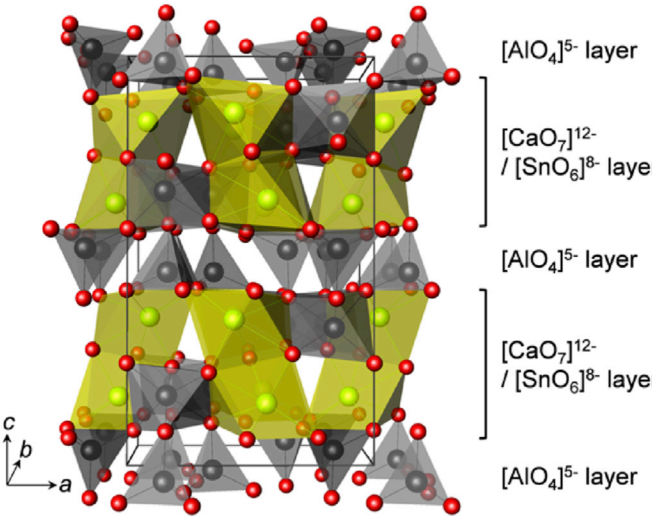

Fig. 1. Crystal structure of $Ca_2Sn_2Al_2O_9$. $[CaO_7]^{12-}$ polyhedra are shown in yellow and a unit cell is indicated by the solid lines. (For interpretation of the references to colour in this figure legend, the reader is referred to the web version of this article.)

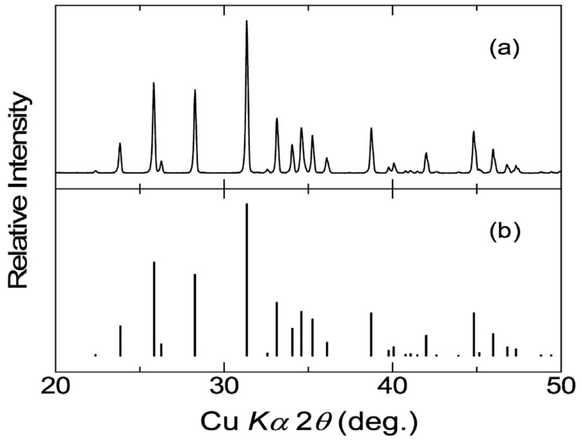

Fig. 2. (a) Powder x-ray diffraction pattern obtained from $(Ca_{1.965}Mn_{0.035})Sn_2Al_2O_9$ and (b) theoretical diffraction pattern of $Ca_2Sn_2Al_2O_9$.

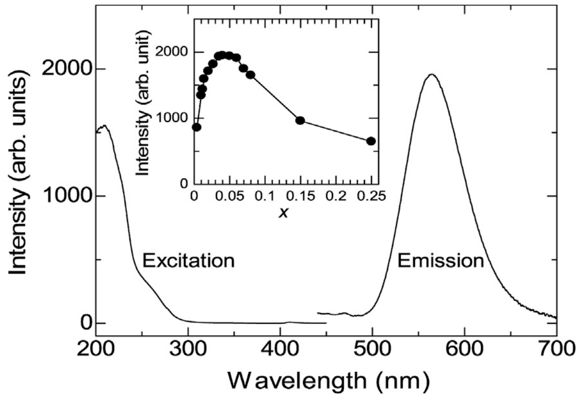

Fig. 3. Excitation and emission spectra of $(Ca_{1.965}Mn_{0.035})Sn_2Al_2O_9$ ($x = 0.035$), acquired at 293 K. The inset shows the emission intensity as a function of Mn^{2+} ion content x.

held at that temperature for several hours with continuous stirring. A resin-like substance was obtained after drying at 423 K, and this material was subsequently heated at 623 K for 3 h to obtain a precursor. After grinding, the precursor was heated at 1673 K for 12 h in air.

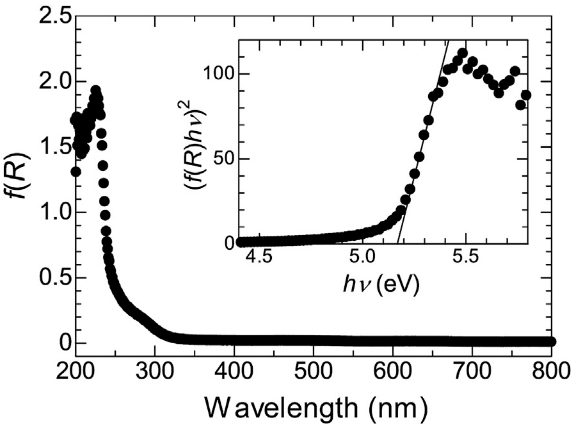

Fig. 4. Optical absorption spectrum of $Ca_2Sn_2Al_2O_9$ ($x = 0$) measured at room temperature. The inset shows a Tauc plot assuming direct allowed transitions.

The crystalline phases were assessed by using powder x-ray diffraction (XRD, RINT2500, Rigaku). The fluorescence properties of the samples were examined between room temperature and 573 K by using a spectrofluorometer (FP-8300, JASCO) equipped with a high-temperature powder-cell unit (HPC-836, JASCO, Japan). All spectra presented herein were calibrated by using rhodamine B (200–360 nm) and a standard halogen light source (360–900 nm, ESC-842, JASCO). As for the $Ca_2Sn_2Al_2O_9$ host, a spectrum of diffuse reflectance R was acquired from 200 to 800 nm by using a spectrophotometer (U-4000, Hitachi) equipped with an integrating sphere, and the Kubelka–Munk conversion $f(R) = (1 - R)^2/(2R)$ was used to obtain an optical absorption spectrum.

3. Results and discussion

Fig. 2(a) presents the powder XRD pattern obtained from $(Ca_{1.965}Mn_{0.035})Sn_2Al_2O_9$ and Fig. 2(b) presents the peaks calculated for the $Ca_2Sn_2Al_2O_9$ host, by using the RIETAN-FP program [21] with the crystallographic parameters refined by Yamane et al. [18]. The measured pattern corresponds well with the calculated peaks. In addition, the XRD patterns of samples with various Mn contents that we synthesized also correspond well with this theoretical pattern, confirming that synthesis by the polymerized complex method provides high-quality samples.

Fig. 3 shows the 293 K excitation and emission spectra for the $(Ca_{1.965}Mn_{0.035})Sn_2Al_2O_9$ sample. A broad emission band centered at 564 nm is apparent, and the intensity of this band reaches a maximum at an excitation wavelength of 210 nm. The emission band has no fine structure, and thus is attributed to Mn^{2+} ions. Calcites ($CaCO_3$) containing Mn^{2+} often exhibit orange fluorescence. As an example, a natural calcite sample examined by Lima et al. [22] fluoresces at 615 nm. In this mineral, the Ca^{2+} ions are surrounded by six O^{2-} ions, and the Ca^{2+}-O^{2-} distance is calculated to be 0.2356 nm based on the crystallographic parameters refined by Chessin et al. [23]. In contrast, when using the crystallographic parameters refined by Yamane et al. [21], the averaged Ca^{2+}-O^{2-} distances are calculated to be 0.2440 nm in the $[CaO_7]^{12-}$ polyhedra in the $Ca_2Sn_2Al_2O_9$ host crystal. As the Mn^{2+}-O^{2-} distance increases, the crystal field generated by the O^{2-} ions surrounding a Mn^{2+} ion weakens, so the Tanabe–Sugano diagram [1] predicts that the emission wavelength will blueshift. Therefore, based on a rough estimate, we attribute the shorter emission wavelength of our samples compared with that of Mn^{2+}-containing calcite to a weaker crystal field around the Mn^{2+} ions in our samples. The inset to Fig. 3 shows the emission intensity as a function of Mn^{2+} content. The intensity rises to a maximum at $x = 0.040$ and subsequently decreases for $x > 0.040$, which may be due to concentration quenching.

Fig. 4 shows the absorption spectrum of $Ca_2Sn_2Al_2O_9$ ($x = 0$) measured at room temperature, which is similar to the absorption spectra from the samples containing Mn ions. In general, absorption by Mn^{2+} is